A petunia ABC protein controls strigolactone-dependent symbiotic signalling and branching

Kretzschmar, Tobias ; Kohlen, Wouter ; Sasse, Joelle ; Borghi, Lorenzo ; Schlegel, Markus ; Bachelier, Julien B ; Reinhardt, Didier ; Bours, Ralph ; Bouwmeester, Harro J ; Martinoia, Enrico

Abstract: Strigolactones were originally identified as stimulators of the germination of root-parasitic weeds that pose a serious threat to resource-limited agriculture. They are mostly exuded from roots and function as signalling compounds in the initiation of arbuscular mycorrhizae, which are plant-fungus symbionts with a global effect on carbon and phosphate cycling. Recently, strigolactones were established to be phytohormones that regulate plant shoot architecture by inhibiting the outgrowth of axillary buds. Despite their importance, it is not known how strigolactones are transported. ATP-binding cassette (ABC) transporters, however, are known to have functions in phytohormone translocation. Here we show that the Petunia hybrida ABC transporter PDR1 has a key role in regulating the development of arbuscular mycorrhizae and axillary branches, by functioning as a cellular strigolactone exporter. P. hybrida pdr1 mutants are defective in strigolactone exudation from their roots, resulting in reduced symbiotic interactions. Above ground, pdr1 mutants have an enhanced branching phenotype, which is indicative of impaired strigolactone allocation. Overexpression of Petunia axillaris PDR1 in Arabidopsis thaliana results in increased tolerance to high concentrations of a synthetic strigolactone, consistent with increased export of strigolactones from the roots. PDR1 is the first known component in strigolactone transport, providing new opportunities for investigating and manipulating strigolactone-dependent processes.

DOI: https://doi.org/10.1038/nature10873

Originally published at:
Kretzschmar, Tobias; Kohlen, Wouter; Sasse, Joelle; Borghi, Lorenzo; Schlegel, Markus; Bachelier, Julien B; Reinhardt, Didier; Bours, Ralph; Bouwmeester, Harro J; Martinoia, Enrico (2012). A petunia ABC protein controls strigolactone-dependent symbiotic signalling and branching. Nature, 483(7389):341-344.
DOI: https://doi.org/10.1038/nature10873

A petunia ABC protein controls strigolactone-dependent symbiotic signaling and branching

Tobias Kretzschmar[1], Wouter Kohlen[2*], Joelle Sasse[1*], Lorenzo Borghi[1], Markus Schlegel[1], Julien B. Bachelier[1], Didier Reinhardt[4], Ralph Bours[2], Harro J. Bouwmeester[2,3] & Enrico Martinoia[1]

[1]Institute of Plant Biology, University of Zurich, 8008 Zurich, Switzerland

[2]Laboratory of Plant Physiology, Wageningen University, 6700 AR Wageningen, The Netherlands

[3]Centre for Biosystems Genomics, P. O. Box 98, 6700 AB Wageningen, The Netherlands

[4]Department of Biology, University Fribourg, 1700 Fribourg, Switzerland

*These authors have contributed equally to this work

Strigolactones were originally identified as germination stimulants of root-parasitic weeds[1] that pose a serious threat to resource-limited agriculture[2]. Primarily they are exuded from roots as signaling compounds involved in the initiation of arbuscular mycorrhiza[3], a mutual plant-fungal symbiosis with global impact on carbon and phosphate cycling[4]. Recently they were established as phytohormones that regulate plant shoot architecture by inhibiting the outgrowth of axillary buds[5,6]. Despite their importance, it is unknown how strigolactones are transported. ATP-binding cassette (ABC) transporters have functions in phytohormone translocation[7-9]. Here we show that the *Petunia hybrida* ABC transporter PhPDR1 plays a key role in regulating arbuscular mycorrhiza and axillary branch development by functioning as a cellular strigolactone exporter. *Phpdr1* mutants are defective in strigolactone exudation from roots, resulting in reduced symbiotic interactions. Aboveground, *phpdr1* exhibits an enhanced branching phenotype, suggestive of impaired

strigolactone allocation. Over-expression of petunia *PDR1* in Arabidopsis results in increased tolerance to high exogenous strigolactone concentrations, consistent with enhanced export from roots. PDR1 is the first known component in strigolactone transport, opening new routes for investigation and manipulation of strigolactone-dependent processes.

Strigolactones (SLs) are a new class of carotenoid-derived[10] phytohormones in land plants. Besides their role in shoot branching, SLs are exuded into the rhizosphere under P-limiting conditions[5] to act as growth stimulants of arbuscular mycorrhizal (AM) fungi[3]. To identify efflux carriers of AM-promoting factors such as SLs, we designed a degenerate primer approach (Supplementary fig. 2a) to isolate full-size ABCG/PDR transporters of petunia abundant in phosphate-starved or mycorrhizal roots. The rationale to focus on ABCG/PDR-type transporters, with 15 members in *Arabidosis*[11], 23 in rice[11] and 23 putative members in tomato (Supplementary fig. 3a), was that they i) are plasma membrane proteins often found in roots[12]; ii) are implicated in belowground plant-microbe interactions[13,14]; iii) have affinities for compounds structurally related to SLs[8,9,15]. Of six primary candidates only *Petunia hybrida PDR1* (*PhPDR1*) displayed enhanced expression in roots subjected to either phosphate starvation (Fig 1a) or colonization by the AM fungus *Glomus intraradices* (Fig. 1b). Furthermore *PhPDR1* transcript levels increased in response to treatments with the synthetic SL analogue GR24 and the auxin analogue 1-naphthaleneacetic acid (NAA) (Fig. 1c). Auxin has been shown to up-regulate SL-biosynthetic genes[16] and to be involved in pre-symbiotic and early mycorrhizal events[17].

PhPDR1 is predicted to encode a full-size ABCG/PDR cluster I protein (GenBank accession: JQ292813, Supplementary fig. 2b-c, Supplementary fig. 3b). The closest *Arabidopsis thaliana* homologue, AtABCG40/AtPDR12, transports abscisic acid (ABA)[9]. However, as opposed to *AtABCG40*, *PhPDR1* is not regulated by ABA (Fig. 1c). A 1.8 kb upstream element of *PhPDR1* (GenBank accession: JQ292814) was fused to the *GUS* reporter and stably transformed into the petunia cultivar W115. Belowground *pPhPDR1::GUS* expression was pronounced in individual sub-epidermal cells of lateral roots (Fig 1d-e). These cells largely overlapped with hypodermal passage cells (HPC) (Fig. 1k-m) that are devoid of suberin and serve as cortical entry points for AM hyphae[18]. GUS staining was more prominent in roots grown under phosphate-deficient conditions (Fig. 1f) and in mycorrhizal roots, particularly in regions containing or flanking fully developed AM structures **(**Fig. 1g-h**)**. These results suggested a role in AM during pre-symbiotic development and during intraradical colonization. For localization the genomic *PDR1* orthologue of the *Petunia hybrida* progenitor *Petunia axillaris*, *PaPDR1* (99.7% amino acid identity to PhPDR1, GenBank accession: JQ292812, Supplementary figure 2b) was C-terminally fused to *GFP* (*GFP::gPaPDR1*). Transient expression of *GFP::gPaPDR1* in *Arabidopsis* showed that PDR1 localizes to the plasma membrane (Fig. 1i-j), consistent with a role in secretion.

For functional analysis we screened the transposon line W138 for insertional *pdr1* mutants. A PCR-based DNA library screen of 1,000 individuals led to the identification of a *dTph1* insertion in exon 4 of *PhPDR1* (Supplementary fig. 4a-d), together with a

78 footprint allele causing a frameshift (Supplementary fig. 4e). Insertion of the *dTph1* in the
79 coding region of a gene frequently results in a complete loss-of-function[19].
80 W138-*pdr1* was compared directly to W138 and crossed with W115 for further
81 segregation analysis. Five homozygous *pdr1* mutant (W115xW138-*pdr1*) and wild-type
82 lines (W115xW138) were derived from the F2 generation (Supplementary fig. 4d).
83 Phenotypes co-segregated with the *PhDR1* mutation and transposon display analysis did
84 not reveal other co-segregating *dTph1* insertions in the W115xW138 lines
85 (Supplementary fig. 4f), suggesting that *dTph1* insertion in *PhPDR1* is responsible for the
86 observed phenotypes. In addition, *PhPDR1* knock-down lines (*phpdr1*-RNAi), created in
87 W115 by use of two independent RNAi constructs (Supplementary fig. 5a-b), exhibited
88 similar phenotypes.
89
90 W138-*pdr1* displayed a significantly reduced ability to accommodate *Gigaspora*
91 *margarita* and *G. intraradices* (Fig 2a), two distantly related AM fungi with different
92 growth strategies[4]. This finding indicated that PDR1 functions as a transporter of a
93 stimulatory molecule involved in symbiosis with diverse AM fungal species. Indeed, root
94 exudates from W138-*pdr1* showed reduced activity to stimulate hyphal branching of *G.*
95 *margarita* in an *in vitro* bioassay (Fig. 2b). As these results suggested an involvement of
96 SLs, W115xW138-*pdr1* root exudates were assessed for their ability to stimulate
97 germination of the root-parasitic weed *Phelipanche ramosa* (Orobanchaceae). As control,
98 root exudates of *dad1* in the petunia cultivar V26 were used. *DAD1* encodes *Carotenoid*
99 *Cleavage Dioxygenase 8* (*CCD8*)[20], an orthologue of the established SL-biosynthetic
100 genes *RMS1*, *MAX4* and *D10* in pea, *Arabidopsis* and rice, respectively[5,6]. The

germination rate of *P. ramosa* was significantly lower with root exudates of W115xW138-*pdr1* and *dad1* compared to exudates of the corresponding wild types, which induced germination to a similar extent as GR24 (Fig. 2d). Comparable results were obtained with *phpdr1*-RNAi lines (Supplementary figure 5c). When inoculated with *G. intraradices*, W115xW138-*pdr1* lines displayed similarly retarded colonization rates as W138-*pdr1* and *dad1* (Fig. 2c). Despite the delay in AM development, neither W115xW138-*pdr1* nor *dad1* displayed any morphological aberrations in intracellular mycorrhizal structures (Fig. 2e-h). Intraradical hyphae and arbuscules appeared normal, suggesting that the quantitative differences in colonization are due to a decreased number of hyphal penetrations and retarded intraradical expansion of AM fungal colonies, rather than to defects in intracellular fungal development. Thus, the phenotype of *dad1* and *phpdr1* was distinct from AM mutants such as *pam1*[21], *str1*[22] or SYM-pathway mutants[4] that commonly exhibit aberrant AM fungal structures.

Detailed analysis of W138 root exudates resulted in the identification of the SL orobanchol (Supplementary figure 6). Orobanchol levels in *phpdr1* root exudates were significantly reduced compared to wild-type plants (Fig. 3a), whereas the levels in root extracts were not affected (Fig. 3b), indicating that *phdr1* is not defective in SL biosynthesis. Orobanchol was detectable neither in root exudates nor in root extracts of *dad1* confirming its supposed defect in SL biosynthesis (Fig. 3a-b). The finding, that only extraradical orobanchol levels were affected in *phdr1*, indicated that PDR1 functions as an SL export carrier.

PDR1-dependent SL transport was further explored in a heterologous system by stable and constitutive over-expression of *GFP::gPaPDR1* in *Arabidopsis* Col-0, resulting in

124 *PDR1*-OE lines (Supplementary fig. 7a-b). *Arabidopsis* does not form AM and exudes
125 only minute quantities of SLs[23]. When grown on GR24-containing medium, *PDR1*-OE
126 lines proved more tolerant to the deleterious effects of high SL concentrations on root
127 elongation[24] than the wild type (Fig. 3c, Supplementary fig. 7c). Direct SL exudation was
128 assessed by quantifying the efflux of pre-loaded ^{3}H-GR24 from roots either incubated at
129 4°C, to monitor passive diffusion, or at 23°C, enabling transporter-mediated efflux. After
130 a period of 1 h *PDR1*-OE roots incubated at 23°C retained significantly less GR24
131 compared to controls at 4°C (Fig. 3d, Supplementary fig. 7d). In agreement with this
132 observation, more GR24 was found in root exudates of *PDR1*-OE lines at 23°C. No
133 significant differences were found for root extracts or root exudates of wild-type or vector
134 control lines in either condition (Fig. 3d). These results together with the observed GR24-
135 resistance phenotype of *PDR1*-OE are best explained with PDR1 acting as an SL
136 exporter.
137 Taken together, our data suggest a role for PDR1 in SL secretion from HPC. We
138 hypothesize that PDR1-mediated SL exudation under low phosphate conditions creates
139 local rhizospheric gradients that guide AM hyphae to HPC, which are susceptible to
140 hyphal penetration (Supplementary fig. 1), thereby initiating AM. The symbiotic
141 phenotype of *phpdr1* and *dad1*, and the induction of *PhPDR1* in colonized root segments
142 suggests that SLs may play an additional role in promoting sustained intercellular root
143 colonization, whereas intracellular stages (*e.g.* arbuscules) develop independently from
144 SLs (Fig. 2e-h).
145 Recently it was demonstrated that SLs inhibit shoot branching[5,6]. Although some aspects
146 of SL biosynthesis and signaling were unraveled[25], information about its mode of

147 transport is scant. SLs are mobile within the xylem sap[23], but it is unknown how they are
148 released from producing cells and whether directed cell-to-cell transport exists. SL
149 biosynthesis is subject to direct negative feedback regulation[26]. Hence SL biosynthesis
150 needs to be coordinated with export to prevent SL accumulation to levels that would
151 restrict further production. Indeed, *PhPDR1* expression was found to be stimulated by
152 exogenous application of GR24 (Fig. 1c and 4a), suggesting substrate-dependent
153 induction, as previously observed for other *ABCG* subfamily[9,15] members.
154 Aboveground *PhPDR1* expression was largely confined to stem tissues, particularly the
155 vasculature and nodal tissues adjacent to leaf axils (Fig. 4b, c). However, *PhPDR1*
156 expression was absent from dormant buds (Fig. 4d). This pattern is consistent with a
157 function of PDR1 as an SL transporter. While SLs are xylem-mobile[23], a cellular
158 transport system is required to deliver SL to dormant buds that are not yet connected to
159 the xylem. This scenario is compatible with both current models for SL-dependent
160 branching control[27]. According to the 'second messenger model', SLs are transported into
161 the bud as a second messenger of auxin[28], hence cellular transport of SL in the axillary
162 regions would be indispensable. In the 'auxin transport canalization-based model' SLs
163 are thought to dampen polar auxin transport, resulting in the accumulation of auxin to
164 levels that inhibit bud outgrowth[29]. SL could restrict auxin transport systemically and/or
165 locally[27]. For both models local SL transport capacity near the axils would be in line with
166 the inhibitory role of SL on branching. In W115xW138-*pdr1,* bud outgrowth was
167 initiated sooner (Supplementary fig. 8a) and more vigorously than in the wild type,
168 causing longer branches (Fig. 4e, Supplementary fig. 8e-h) at node three to five. This was
169 also observed in *phpdr1*-RNAi lines (Fig. 4f). *Dad1* initiates branches from all nodes

(Supplementary fig. 8d), and though branch elongation is retarded, it eventually produces full branches from every node[20,30]. At flowering time this results in a phenotype that is more pronounced than in any of the *phpdr1* mutants, which display final branch patterns that differ only marginally from the respective wild types (Supplementary fig. 8b-c, Supplementary table 1). Nevertheless the *phpdr1* branching phenotype appears SL-dependent and related to the *dad1* branching phenotype, as branch elongation in both mutants could be suppressed to near wild-type conditions by exogenous application of GR24 to the leaf axils (Fig. 4 g-h).

In conclusion, the identification of PDR1-mediated SL transport contributes to a more comprehensive view of SL modes of action. Understanding the underlying transport mechanisms is crucial for a holistic view of phytohormone function. SL transport has direct impact on phosphate-dependent control of AM levels and on control of shoot branching, where the integration of auxin and SL signaling seems partially achieved through reciprocal transport modulation. The mild branching phenotype of *phpdr1* relative to the SL biosynthetic mutant *dad1*[30] suggests that residual transport and/or locally produced SLs may compensate for defective SL transport in the shoot. However, AM development was affected to a similar degree in *phpdr1* and *dad1*, revealing that belowground SL transport and secretion relies primarily on PDR1.

Methods summary:

All experiments with exception of transport assays were performed in accordance with established protocols. Detailed methods and associated references can be found online as supplementary information.

Acknowledgements:

We kindly thank: C. Gübeli for technical assistance; T. Gerats, S. Hörtensteiner, A. Osbourne, P. Schläpfer and C. Beveridge for comments. This study was funded by the Swiss National Foundation within the NCCR-Plant Survival, the project "ABC transporters involved in signaling" and by The Netherlands Organization for Scientific Research (NWO; VICI grant, 865.06.002 and Equipment grant, 834.08.001to H.B.). H.B. was co-financed by the Centre for BioSystems Genomics (CBSG).

Author contributions:

T.K. wrote the manuscript, designed the project and carried out most of the experiments. W.K. and R.B. carried out the LC-MS/MS analysis and the *P. ramosa* biossays. J.S. performed qRT analysis and transport. J.S. and M.S. performed branching and GUS trials. L.B. analyzed *PDR1*-OE lines. J.B. sectioned material. D.R. investigated AM morphology. H.B. supervised the analytical part of the project. E.M. conceived and supervised the project. DR, EM, JS, WK and HB assisted in editing.

REFERENCE LIST:

1. Cook, C. E., Whichard, L. P., Turner, B., Wall, M. E. & Egley, G. H. Germination of Witchweed (Striga lutea Lour.): Isolation and Properties of a Potent Stimulant. *Science* **154**, 1189-1190 (1966).
2. Yoder, J. I. & Scholes, J. D. Host plant resistance to parasitic weeds; recent progress and bottlenecks. *Current Opinion in Plant Biology* **13**, 478-484 (2010).
3. Akiyama, K., Matsuzaki, K.-i. & Hayashi, H. Plant sesquiterpenes induce hyphal branching in arbuscular mycorrhizal fungi. *Nature* **435**, 824-827 (2005).

4. Parniske, M. Arbuscular mycorrhiza: the mother of plant root endosymbioses. *Nat Rev Microbiol* **6**, 763-775 (2008).
5. Umehara, M. et al. Inhibition of shoot branching by new terpenoid plant hormones. *Nature* **455**, 195-200 (2008).
6. Gomez-Roldan, V. et al. Strigolactone inhibition of shoot branching. *Nature* **455**, 189-194 (2008).
7. Petrasek, J. & Friml, J. Auxin transport routes in plant development. *Development* **136**, 2675-2688 (2009).
8. Kuromori, T. et al. ABC transporter AtABCG25 is involved in abscisic acid transport and responses. *Proc Natl Acad Sci U S A* **107**, 2361-2366 (2010).
9. Kang, J. et al. PDR-type ABC transporter mediates cellular uptake of the phytohormone abscisic acid. *Proc Natl Acad Sci U S A* **107**, 2355-2360 (2010).
10. Matusova, R. et al. The strigolactone germination stimulants of the plant-parasitic Striga and Orobanche spp. are derived from the carotenoid pathway. *Plant Physiol* **139**, 920-934 (2005).
11. Verrier, P. J. et al. Plant ABC proteins--a unified nomenclature and updated inventory. *Trends Plant Sci* **13**, 151-159 (2008).
12. Moons, A. Transcriptional profiling of the PDR gene family in rice roots in response to plant growth regulators, redox perturbations and weak organic acid stresses. *Planta* **229**, 53-71 (2008).
13. Badri, D. V. et al. An ABC transporter mutation alters root exudation of phytochemicals that provoke an overhaul of natural soil microbiota. *Plant Physiol* **151**, 2006-2017 (2009).
14. Sugiyama, A., Shitan, N. & Yazaki, K. Signaling from soybean roots to rhizobium: An ATP-binding cassette-type transporter mediates genistein secretion. *Plant Signal Behav* **3**, 38-40 (2008).
15. Jasinski, M. et al. A plant plasma membrane ATP binding cassette-type transporter is involved in antifungal terpenoid secretion. *Plant Cell* **13**, 1095-1107 (2001).
16. Hayward, A., Stirnberg, P., Beveridge, C. & Leyser, O. Interactions between auxin and strigolactone in shoot branching control. *Plant Physiol* **151**, 400-412 (2009).
17. Hanlon, M. T. & Coenen, C. Genetic evidence for auxin involvement in arbuscular mycorrhiza initiation. *New Phytologist* **189**, 701-709 (2011).
18. Sharda, J. N. & Koide, R. T. Can hypodermal passage cell distribution limit root penetration by mycorrhizal fungi? *New Phytologist* **180**, 696-701 (2008).
19. Koes, R. et al. Targeted gene inactivation in petunia by PCR-based selection of transposon insertion mutants. *Proc Natl Acad Sci U S A* **92**, 8149-8153 (1995).
20. Snowden, K. C. et al. The Decreased apical dominance1/Petunia hybrida CAROTENOID CLEAVAGE DIOXYGENASE8 gene affects branch production and plays a role in leaf senescence, root growth, and flower development. *Plant Cell* **17**, 746-759 (2005).
21. Reddy D M R, S., Schorderet, M., Feller, U. & Reinhardt, D. A petunia mutant affected in intracellular accommodation and morphogenesis of arbuscular mycorrhizal fungi. *Plant J* **51**, 739-750 (2007).

22. Zhang, Q., Blaylock, L. A. & Harrison, M. J. Two Medicago truncatula half-ABC transporters are essential for arbuscule development in arbuscular mycorrhizal symbiosis. *Plant Cell* **22**, 1483-1497 (2010).
23. Kohlen, W. et al. Strigolactones are transported through the xylem and play a key role in shoot architectural response to phosphate deficiency in nonarbuscular mycorrhizal host Arabidopsis. *Plant Physiol* **155**, 974-987 (2011).
24. Ruyter-Spira, C. et al. Physiological effects of the synthetic strigolactone analog GR24 on root system architecture in Arabidopsis: another belowground role for strigolactones? *Plant Physiol* **155**, 721-734 (2011).
25. Beveridge, C. A. & Kyozuka, J. New genes in the strigolactone-related shoot branching pathway. *Curr Opin Plant Biol* **13**, 34-39 (2010).
26. Mashiguchi, K. et al. Feedback-regulation of strigolactone biosynthetic genes and strigolactone-regulated genes in Arabidopsis. *Biosci Biotechnol Biochem* **73**, 2460-2465 (2009).
27. Domagalska, M. A. & Leyser, O. Signal integration in the control of shoot branching. *Nat Rev Mol Cell Biol* **12**, 211-221 (2011).
28. Brewer, P. B., Dun, E. A., Ferguson, B. J., Rameau, C. & Beveridge, C. A. Strigolactone Acts Downstream of Auxin to Regulate Bud Outgrowth in Pea and Arabidopsis. *Plant Physiol.* **150**, 482-493 (2009).
29. Crawford, S. et al. Strigolactones enhance competition between shoot branches by dampening auxin transport. *Development* **137**, 2905-2913 (2010).
30. Napoli, C. Highly Branched Phenotype of the Petunia dad1-1 Mutant Is Reversed by Grafting. *Plant Physiol* **111**, 27-37 (1996).

Figure legends:

Figure 1 | Belowground *PhPDR1* expression and PDR1 localization
a-c, qPCR for *PhPDR1* in W115 roots; in presence or absence of phosphate (P) (**a**); 2-4 weeks post inoculation (wpi) with *G. intraradices* (**b**); in response to H_2O, GR24, NAA, ABA (**c**); means ± s.e.m. (N = 3). **d-h**, *pPhPDR1::GUS* signal in W115 roots without treatment (E: epidermal cell) (**d-e**); under P-sufficient and P-deficient conditions (**f**); in response to mycorrhization (+MYC = 8 wpi) (**g**) in mycorrhized roots (8 wpi) co-stained with black ink (black arrows; mycorrhized sections) (**h**). Scale bars = 1 mm (e: 0.1 mm). **i-j**, Transient *CaMV 35S::GFP-gPaPDR1* expression in *Arabidopsis* mesophyll protoplasts. GFP- gPaPDR1 signal and corresponding transmission image (**i**) and free GFP signal and transmission image (**j**). Scale bar = 10 µm. **k-m**, *pPhPDR1::GUS* signal co-localization with trypan blue stained root hypodermal passage cells. Magenta GUS stained root section (**k**); additional trypan blue stain of the same sample (**l**) and stained wild-type (**m**). Scale bars = 0.1 mm.

Figure 2 | Belowground *phpdr1* phenotypes
a, AM colonization of W138 and W138-*pdr1* roots 8 wpi with two AM fungi, means ± s.e.m. (N > 20). **b**, *In vitro* branching response of *G. margarita* 24 h after GR24 application (N = 5), root exudates of W138 (N = 17), W138-*pdr1* (N = 36) or 10% acetone (solvent, N = 5), means ± s.e.m.. **c**, Kinetics of *G. intraradices* colonization of W115xW138 (N = 25), W115xW138-*pdr1* (N = 25), V26 (N = 5) *dad1* (N = 5), means ± s.e.m. ($p < 0.001$ for all time points between mutants and wild-types). **d**, *P. ramosa* germination induced by GR24 (N = 3), root exudates of W115xW138 (WxW WT, N = 10), W115xW138-*pdr1* (WxW *pdr1*, N = 10), V26 (N = 4), *dad1* (N = 4) or water (N = 4), means ± s.e.m.. **e-h**, *G. intraradices* intracellular AM morphology 4 wpi in W115xW138 (**e**); W115xW138-*pdr1* (**f**); V26 (**g**) and *dad1* (**h**). Scale bars = 20 µm. * = $p < 0.05$; *** = $p < 0.001$ in all panels

Figure 3| Orobanchol contents and PDR1-dependent GR24 tolerance and transport
a-b Orobanchol in the root exudates (**a**) and extracts (**b**) of *Phpdr1* lines, *dad1* and wild-types (N = 9), means ± s.e.m. **c**, Col-0 and *PDR1*-OE grown on 0, 10, and 25 µM GR24. Scale bar = 1 cm **d**, Export assay of ^{3}H-GR24 preloaded roots of Col-0, vector control (VC) and *PDR1*-OE lines (OE L1-3). Relative ^{3}H-GR24 in the medium (water), root and shoot, after 1 hour incubation at 4°C and 23°C; means ± s.e.m. (N = 8). * = $p < 0.05$; *** = $p < 0.001$ in all panels.

Figure 4 | Aboveground *PhPDR1* expression and *phpdr1*-related branching phenotypes
a-b, qPCR for aboveground W115 GR24-treated tissue (**a**) and different organs (**b**);. means ± s.e.m. (N = 3). **c-d**, *pPhPDR1::GUS* in W115 at the four-leaf stage (**c**) and a node close-up (**d**) (white arrow: dormant axillary bud). Scale bars: b = 10 mm; d = 1 mm. **e-f**, Branch development 41 days post germination (dpg); means ± s.e.m., Branch length for W115xW138 and W115xW138- *pdr1* (N = 110) **(e)** and for W115 and two *Phpdr1*-RNAi lines, R104 ($p < 0.001$ for node 3-4), and C244 ($p < 0.05$ for node 3)

(N=8) (**f**). **g-h**, Effects of GR24 (striped) on branch development 34 dpg at node 3-5 for W115xW135 and W115xW138-*pdr1* (N = 24), (**g**) V26 and *dad1* (N = 8) (**h);** means ± s.e.m. *=p<0.05;***=p<0.001 in all panels

Methods and materials (supplementary online information):

1 Plant growth conditions

Petunia lines were grown at 16 h light, 60% relative humidity and 25°C in soil (ED 73 Einheitserde, Einheitserde Werksverband e.V., Germany) or in clay granules (Oil Dry US Special, Damolin, Switzerland). Clay granules were supplemented once a week with half-strength Hoagland solution. For mycorrhization trials a mix of 40% [v/v] soil, 40% [v/v] clay granules, 10% [v/v] sand and 10% [v/v] mycorrhizal inoculum (AGRAUXINE, France) was used. Seeds were plated on medium containing 2.2 g L^{-1} MS (Duchefa, The Netherlands) and 15 g L^{-1} sucrose, supplemented with 9 g L^{-1} PHYTO AGAR (Duchefa, The Netherlands) at 16 h of light and 25°C. *Arabidopsis thaliana* was grown in vertical plates on medium containing 2.2 g L^{-1} MS (Duchefa, The Netherlands) and 15 g L^{-1} sucrose, supplemented with 9 g L^{-1} PHYTO AGAR (Duchefa, The Netherlands) at 16 h light, 60% relative humidity and 21°C. For hormone treatment 14 d old W115 seedlings grown on plate were exposed for 24 h with final concentrations of 1 or 10 µM of the synthetic SL analog GR24 (Chiralix, The Netherlands), 10 µM abscisic acid (ABA) or 25 µM 1-naphthaleneacetic acid (NAA). For phosphate starvation 14 d old W115 seedlings were transferred to P-free plates for one week.

2 *PDR1* cloning strategy

PDR-specific 0.5 kb transcripts were amplified from W115 root cDNA five wpi with *G. intraradices* with: 5`-mgwatgactctdytkytkggacctcc and 5`-gyttcytytgncchcchgaaatwcc (5`region) or with: 5`-gggwaaracggwgtyagtggwgcw and 5`-ctcatnacaatdgcwgcwgctctwgc (3`region). Resulting 5` and 3` fragments were aligned and the deduced consensus primers 5`-tattgggacttgaaatttgtgccgatac and 5`-gctccactaacacccatcagagctgtc were used to amplify putative *PDR* fragments spanning 2.5 kb. 5` and 3` ends of *PhPDR1* were amplified using the SMART-RACE Amplification Kit (Clontech, Takara Bio Company, USA) with 5`RACE 5'-ctcgagtacattttctcggggaccttgg, nested 5`RACE 5'-ccatttcgtctccaacaatggtatcgg, 3`RACE 5'-gtcctcaagagtaggaagcatcactgcg and nested 3`RACE 5'-accgaggaccggcttgaactcttgagag. Full length *PhPDR1* cDNA GenBank accession is JQ292813.

To obtain the full length genomic sequence of *PDR1* a *Petunia axillaris* BAC library (kind gift of Chris Kuhlemeier, University of Bern) was screened with: 5'-tgccaatccttcatgatgtcagtgg and 5'-ccttctctctcctagacagctctgc. *P. axillaris* is a progenitor of the hybrid species *P. hybrida*[31] and a genomic library for BAC-based cloning was only available for the former. BACs were extracted from candidate clones via the Large Constuct Kit (Qiagen, Germany). Full length genomic *PaPDR1* was amplified from BAC with 5'-aattactagtatggagggtggtgaag and 5'-aattgcatgcctatcttttctggaaattaaatg cut with SpeI and SphI and cloned into pUC18-GFP5sp via compatible *Nhe*I and *Sph*I restriction sites for GFP localization studies[32]. For stable transformation the *CaMV 35S*::*GFP::gPaPDR1-terminator* cassette was cloned from pUC18-GFP5sp into pGreenII0179 vector[33] via the following strategy: i) The *CaMV 35S* promoter from native pUC18-GFP5sp was cloned via *Xho*I and *Xma*I. ii) The terminator from the native pUC18-GFP5sp including the upstream *Sph*I site was cut with NheI and SacI and inserted into *CaMV 35S* -pGreenII0179 via compatible *Xba*I and *Sac*I sites. iii) *GFP::gPaPDR1* was cut and cloned via *Xma*I and *Sph*1. 9 kb of the genomic *PaPDR1* locus, including upstream and downstream sequence, are submitted with GenBank under accession JQ292812.

3 *PhPDR1* promoter GUS construct and GUS staining assay

A 1.8 kb *PhPDR1* promoter fragment was amplified using the Genome Walker Universal Kit (Clontech, Takara Bio Company, USA) with 5`-agttggaagtttctcaagtgcagccca and the nested 5`-ccctaaagagttcttcaccaccctccat (GenBank accession JQ292814). The fragment was cloned into the pGEM-T-Easy vector system (Promega, USA), reamplified with 5'-catgaagcttgcacccagaagaagattaggc and 5'-tcgatctagacacattaagaggaaagtaggtac and cloned into the pGPTV-Bar[34] vector system via *Hind*III and *Xba*I. Of the original T0 transformants eight lines were selected for further analysis. Segregating T1 individuals of all eight lines displayed comparable belowground and aboveground expression patterns at different developmental stages. Two of these lines were chosen for the in depth analysis presented in this work and all data presented was confirmed in both lines.

GUS-staining trials were performed as described previously[35]. After staining, samples were cleared for 24 h in 10% [w/v] KOH and stored in 70% [v/v] ethanol. For analysis of

463 hypodermal passage cells, 5-bromo-6-chloro-3-indolyl β-D-glucuronide
464 cyclohexylammonium salt was used for GUS staining and samples were cleared for 24 h
465 in 10% [w/v] KOH before staining with trypan blue as described[18].
466
467 **4 *PhPDR1* RNA interference constructs**
468 Silencing of *PhPDR1*-specific transcripts was performed with the pKANNIBAL vector
469 system[36]. Two constructs were designed, one targeting a highly variable region within the
470 nucleotide binding domain 2 (NBD2) of *PhPDR1* (C-construct) and one targeting a part
471 of the 3`end and the 3`UTR of *PhPDR1* (R-construct). The 148 bp C-fragment
472 (ggaacgcaagcaaaaggggtgaggttattgaactatcttcgcttggaaagagctcttctgaaaaaggaaatgatgttcggcgaa
473 gtgcatcttccaggtcaatgtcctcaagagtaggaagcatcactgcggctgatttgagcaagag) was amplified from
474 W115 cDNA with 5'-cgatggatcctcgagggaacgcaagcaaaaggg, containing *BamH*I and *Xho*I
475 restriction sites and 5'-cgatatcgatggtaccctcttgctcaaatcagccgcagtga containing *Cla*I and
476 *Kpn*I sites. The 411 bp R-fragment (gacattatatggactaattgcctcacaatttggagacatacaagacag
477 acttgacacaaatgagacagtggaacaattcatagagaatttctttgatttcaaacatgattttgtgggatatgttgctctcattcttgtt
478 gggatttctgttctttttctcttcatttttgcattttcaattaaaacatttaatttccagaaaagataggttggtccaggtatacacatgaaa
479 agagcgtttatcaagatatgtgtatattaggataataatataatctttctttttcctctttttacttattgtggttttctcaagtttggaataga
480 tagaaccaaaagtctgtactctgtatttaagaacaacttttgtacacattgttatgtattggagaagttatgagtatcttttg) was
481 amplified with 5`cgatggatcctcgagacattatatggactaattgcc, containing *BamH*I and *Xho*I
482 restriction sites and 5`cgatatcgatggtaccaaaagatactcataacttctcc containing *Cla*I and *Kpn*I
483 sites. The resulting amplicons were cloned in sense and antisense direction in the two
484 multiple cloning sites of pKANNIBAL. The pKANNIBAL RNAi cassette was excised
485 from the vector backbone via *Not*I and transferred into the binary pGreenII0229 vector[33].
486 After stable transformation of W115 the extent of down-regulation was estimated via
487 semi-quantitative PCR or RT-PCR.
488
489 **5 Plant transformation**
490 W115 was transformed as described[37]. Construct insertion was confirmed via PCR on
491 genomic DNA with 5'-acggtccacatgccggtatatacgatg and 5'-gatggcatttgtaggagccaccttcc,
492 targeting the CaMV35S promoter, or with 5'-gaattgatcagcgttggtgggaaagc and 5'-
493 ggtaatgcgaggtacggtaggagttg, targeting the GUS gene.

Transient transformation of *Arabidopsis thaliana* Col-0 protoplasts was performed as described previously[32]. Arabidopsis plants were stably transformed as described[38]. T0 generation was selected for hygromycin resistance. Plants of the T1 generation were tested for hygromycin resistance and GFP expression.

6 Screening approach to identify transposon insertions in *PhPDR1*

A 3D-gDNA library (kind gift from Tom Gerats, Radboud University, Nijmegen) representing 10x10x10 (1,000) W138 individuals was screened for *dTph1* insertions in *PhPDR1* via a PCR-based method[39]. The entire genomic region of *PhPDR1* was scanned in contiguous steps covering less than 1 kb, using the *dTph1*-specific primer 5`-gaattcgctccgcccctg and a variety of ^{33}P-labeled gene-specific primers. The primer 5'-ccatttcgtctccaacaatggtatcgg yielded a positive result. Homozygosity PCRs were performed with the transposon flanking primers: 5'-tgccaatccttcatgatgtcagtgg and 5'-ccttctctctcctagacagctctgc. Homozygous *dTph1* insertion alleles were furthermore crossed into W115, the progeny selfed and the resulting offspring tested for homozygosity with the above mentioned primers. Transposon display analysis utilizing six W115xW138 and five W115xW138-*pdr1* lines was performed as described[40].

7 Mycorrhization trials

Subsets of mycorrhized roots were stained[41] and quantified for their level of colonization using the gridline intersect method[42]. Only the presence of clear intraradical structures such as coiled cortical hyphae, arbuscles and vesicles were scored as positively mycorrhized. A minimum of 200 intersecting root fragments per sample were investigated microscopically for intraradical AM structures. For trials involving W115xW1138 lines 5 individuals of 5 lines were analysed and the data presented as a pool of N=25 (5x5). Double staining of colonized roots with propidium iodide and wheat germ agglutinin coupled to fluorescein isothiocyanate (WGA-FITC; Sigma-Aldrich) was performed as described[43].

8 Hyphal branching bioassays

Branching assays were performed as previously described[44] with pre-selected spores of *Gigaspora margarita* (AGRAUXINE, France). For production of the root exudates concentrate, petunia lines were grown in clay granules and were transferred for 24 h to 0.1 L of a hydroponic solution containing 2 mM $CaCl_2$ and 2 mM KSO_4 and kept under constant aeration. The hydroponic solution was then run through a Sep-Pak Classic C18 Cartridge (Waters, Ireland) to adsorb hydrophobic root exudates. Exudates were eluted from the column using 2 ml of acetone and the eluent was dried over nitrogen. Dried exudates were re-dissolved in acetone and normalized according to root fresh weight (FW). Exudate equivalents of 10 mg root FW were used in each branching assay.

9 Transport assays and GR24 tolerance assays

Arabidopsis seeds of three independent *PDR1*-OE lines were surface-sterilized with 1% [v/v] bleach and 50% [v/v] ethanol and plated on media supplemented with 2.2 g L^{-1} MS, 1% [w/v] sucrose and 0, 10, or 25 µM GR24. After three days of stratification plants were moved to a 16 h light /8 h dark regime and selected for GFP fluorescence after 3 days of growth. Root length was determined with the ImageJ 1.44 software (http://rsbweb.nih.gov/ij) after seven days and seedlings were moved to hygromycin-containing plates without sucrose to confirm the selection by GFP fluorescence.

For transport experiments, seeds were sterilized in the same way and plated on hygromycin-containing media. After three days of stratification and three days of growth, seedlings were checked for GFP fluorescence. After seven days, GFP- and hygromycin-positive plants were transferred to media supplemented with 2.2 g L^{-1} MS, 1% [w/v] sucrose and grown for another seven days. Three *PDR1*-OE lines, Col-0 and a vector control line were incubated for 2 h in the dark at 4°C with root tips submerged in 0.1% [w/v] Phytoagar (Duchefa Biochemie, The Netherlands) supplemented with 25 nM ^{3}H-GR24 (specific activity 40 Ci $mmol^{-1}$, American Radiolabeled Chemicals, USA). Subsequently, the plant roots were washed in ice-cold 1 mM $CaCl_2$ and incubated in 200 µl 0.1% Phytoagar. For each line, 50% of the plants were further kept for 1 h at 4°C in the dark as diffusion control, the other 50% were shifted for 1 h to 23°C to monitor transport. Subsequently, shoot, root and Phytoagar fractions were incubated for 30 min in 50 µl 24% [w/v] trichloroacetic acid at 23°C. Tritium counts were determined in 3 ml

555 Ultima Gold LSC cocktail (Perkin Elmer, USA) with Liquid Scintillation Analyzer Tri-
556 Carb 2900TR (Packard BioScience, USA). Disintegrations per minute (dpm's) were
557 computed into percentages for each fraction and normalized to tissue fresh weights.
558
559
560 **10 RNA isolation, cDNA synthesis, semi-quantitative PCR and quantitative RT-**
561 **PCR**
562 RNA was isolated with the RNeasy Plant Mini Kit (Qiagen, Germany). Reverse
563 transcription of RNA to cDNA was performed with the M-MLV reverse transcriptase
564 (Promega, USA) and a polyT primer (Promega, USA).
565 *PhPDR1* expression was quantified semi-quantitatively with 5'-gaaactgtggccgaaagg and
566 5'-gagttcaagccggtcct or 5`-aaatgctactacagtgcag and 5`-catataatgtccaggaaatggg. Tubulin1
567 transcript (*PhTUB*), partially amplified with 5`-cattggtcaagccggttattc and 5`-
568 acccttgaagaccagtacagt served as housekeeping and loading control.
569 Samples were diluted 1:30, and 4µl of the dilutions were added to each reaction well,
570 serving as template for the reaction. Deionized water served as negative control for
571 amplification. *PhPDR1* expression was quantified with 5'-cctgaggtttaccaaatggg and
572 5'gatggtattggattggagca. *Glyceraldehyde 3-phosphate dehydrogenase* (*GapDH*) expression
573 was quantified with 5'-gactggagaggtggaagagc and 5'-ccgttaagagctgggagaac. *GapDH*
574 served as housekeeping gene for normalization because it was shown to be not regulated
575 by hormonal treatments or mycorrhization (Didier Reinhardt, personal communication).
576 Final primer concentrations of 50, 100, 200, and 300 nM were tested for cDNA
577 amplification and melting behaviour in a range of 60°C – 95°C. Because no differences
578 were recorded, the average concentration of 100 nM was chosen for further experiments.
579 Primer efficiency was recorded with W115 root cDNA as template in a dilution range of
580 1:1 – 1:512, resulting in 94.42% for *PhPDR1* and 98.561% for *GapDH*. These values
581 were taken into account in the calculations. Sybr Green PCR Master Mix (Applied
582 Biosystems) was added to the samples to a final volume of 20 µl. For each sample, three
583 technical replicates were pipetted. RT-PCR was performed on a 7500 Fast Real-Time
584 PCR System (Applied Biosystems) with the 7500 Software v2.0.4. The Quantitation-
585 Comparative CT (ΔΔCT) was chosen as method[45], the PCR run was divided into three

parts: 1. Hold stage (50°C for 2 min, 95°C for 10 min); 2. Cycling stage (95°C 15 s, 60°C 1 min for 40 cycles); Melt Curve stage (95°C 15 s, 60°C to 95°C 1 min, 95°C 30 s, 60°C 15 s). Relative differences were calculated as described[45,46]. Each experiment was performed for three biological replicates.

11 Isolation, identification and quantification of petunia strigolactones

Plants were grown in a X-stream 20 aeroponic system (Nutriculture, UK) as previously described for *Medicago truncatula*[47]. From day eight until day twelve exudates were collected, pooled and root material sampled and stored at -80°C for further analysis. *P. hybrida* root exudates and extracts were prepared and analyzed by ultra performance liquid chromatography coupled to tandem mass spectrometry (UPLC-MS/MS) as previously described for Arabidopsis[22]. Orobanchol was kindly provided by Koichi Yoneyama (Weed Science Center, Utsunomiya University, Japan). For trials involving W115xW1138 lines 3 individuals of 3 lines were analyzed and the data presented as a pool of N = 9 (3x3).

12 *Phelipanche ramosa* germination bioassay

Germination assays with *P. ramosa* seeds were conducted as reported previously[10]. Exudates were prepared as in **8**. GR24 at 1 and 0.1 nM and demineralised water were included as positive and negative controls. *P. ramosa* seeds were kindly provided by Maurizio Vurro (Istituto di Scienze delle Produzioni Alimentari, Italy). For trials involving W115xW1138 lines 2 individuals of 5 lines were analyzed and the data presented as a pool of N = 10 (5x2).

13 Trypan blue staining of hypodermal passage cells

Trypan blue stains of hypodermal passage cells in roots were performed as described[18].

14 Axillary branching trials

For a comparative analysis of lateral branch production in wild type and *pdr1* backgrounds, plants were grown for 65 d in 0.55 L pots in soil as described in **1** and

617 watered daily. Branch development was monitored at different time points in a binominal
618 fashion (yes/no) in respect to the following parameters: bud length > 7 mm; full branch.
619 Full branches were scored in accordance to a petunia branch definition[48]. Furthermore
620 branch length was scored as a continuous parameter. For trials involving W115xW1138
621 22 individuals of 5 lines were analyzed and the data presented as a pool of N = 110
622 (5x22). For branch length trials in response to GR24 treatments three lines each of
623 W115xW135, W115xW138-*pdr1*, V26, and *dad1* (kind gift of Kimberly Snowden, New
624 Zealand Institute for Plant and Food Research Limited, Auckland) were grown on soil as
625 described in **1**. From 25 - 40 dpg, plants were treated three times each week with 0 µM or
626 10 µM GR24 as described[6]. For trials involving W115xW1138 lines 8 individuals of 3
627 lines were analyzed and the data presented as a pool of N = 24 (3x8).
628
629 **15 Statistical analyses**
630 Depending on experimental set-ups and prerequisites Students t-tests, Fishers Exact tests
631 or generalized linear models (GLM) with quasi-binominal error structures were applied
632 using the "R" software (R Development Core Team 2009).
633
634 **16 Bioinformatics**
635 Analysis of DNA fragments and vector constructs was performed using VectorNTI
636 (Invitrogen). Membrane topology of PhPDR1 was predicted using ConPredII
637 (*bioinfo.si.hirosaki-u.ac.jp/~ConPred2/*). Phylogenetic analysis of PhPDR1 was
638 performed using tools available at phylogeny.fr (www.phylogeny.fr). Alignments were
639 performed with Multalin (***multalin***.*toulouse.inra.fr/****multalin****/*).
640
641 **17 Robustness of data sets**
642 All data sets presented were confirmed in at least two independent trials with similar set-
643 ups and outcomes. For mycorrhization and branching trials individual pots were
644 randomized to reduce positional effects and sample size was kept high to reduce
645 background effects.
646
647

References:

31. Zhang, X., Nakamura, I. & Mii, M. Molecular Evidence for Progenitorial Species of Garden Petunias Using Polymerase Chain Reaction-Restriction Fragment Length Polymorphism Analysis of the Chs-j Gene *HortScience* **43** 300-303 (2008).
32. Meyer, A., Eskandari, S., Grallath, S. & Rentsch, D. AtGAT1, a high affinity transporter for γ-aminobutyric acid in Arabidopsis thaliana. *Journal of Biological Chemistry* **281** 7197-7204 (2006).
33. Hellens, R. P., Edwards, E. A., Leyland, N. R., Bean, S. & Mullineaux, P. M. pGreen: a versatile and flexible binary Ti vector for Agrobacterium-mediated plant transformation. *Plant Mol Biol* **42**, 819-832 (2000).
34. Becker, D., Kemper, E., Schell, J. & Masterson, R. New plant binary vectors with selectable markers located proximal to the left T-DNA border. *Plant Mol Biol* **20**, 1195-1197 (1992).
35. Cervera, M. Histochemical and fluorometric assays for uidA (GUS) gene detection. *Transgenic Plants: Methods and Protocols* **286**. 203-213 (2004).
36. Wesley, S. V. et al. Construct design for efficient, effective and high-throughput gene silencing in plants. *Plant J* **27**, 581-590 (2001).
37. Lutke, W. K. Petunia (Petunia hybrida). *Methods Mol Biol* **344**, 339-349 (2006).
38. Harrison, S. et al. A rapid and robust method of identifying transformed Arabidopsis thaliana seedlings following floral dip transformation. *Plant Methods* **2**, 19 (2006).
39. Vandenbussche, M. & Gerats, T. TE-based mutagenesis systems in plants: a gene family approach. *Methods Mol Biol* **260**, 115-127 (2004).
40. Van den Broeck, D. et al. Transposon Display identifies individual transposable elements in high copy number lines. *Plant J* **13**, 121-129 (1998).
41. Vierheilig, H., Coughlan, A., Wyss, U. & Piche, Y. Ink and vinegar, a simple staining technique for arbuscular-mycorrhizal fungi. *Appl Environ Microbiol* **64**, 5004-5007 (1998).
42. Giovannetti, M. & Mosse, B. An Evaluation of Techniques for Measuring Vesicular Arbuscular Mycorrhizal Infection in Roots. *New Phytologist* **84**, 489-500.
43. Feddermann, N. et al. The PAM1 gene of petunia, required for intracellular accommodation and morphogenesis of arbuscular mycorrhizal fungi, encodes a homologue of VAPYRIN. *Plant J* **64**, 470-481 (2010).
44. Nagahashi, G. & Douds, D. D. Rapid and sensitive bioassay to study signals between root exudates and arbuscular mycorrhizal fungi. *Biotechnology Techniques* **13**, 893-897 (1999).
45. Livak, K. J. & Schmittgen, T. D. Analysis of relative gene expression data using real-time quantitative PCR and the 2(-Delta Delta C(T)) Method. *Methods* **25**, 402-408 (2001).
46. Yuan, J. S., Reed, A., Chen, F. & Stewart, C. N. Statistical analysis of real-time PCR data. *BMC Bioinformatics* **7**, 85 (2006).

47. Liu W. et al. Strigolactone biosynthesis requires the symbiotic GRAS-TYPE transcription NSP1 and NSP2. *Plant Cell* (2011) [epub ahead of print, doi: 10.1105/tpc.111.089771]
48. Snowden, K. C. & Napoli, C. A. A quantitative study of lateral branching in petunia. *Functional Plant Biology* **30**, 987-994 (2003/01/01).

Figure 1

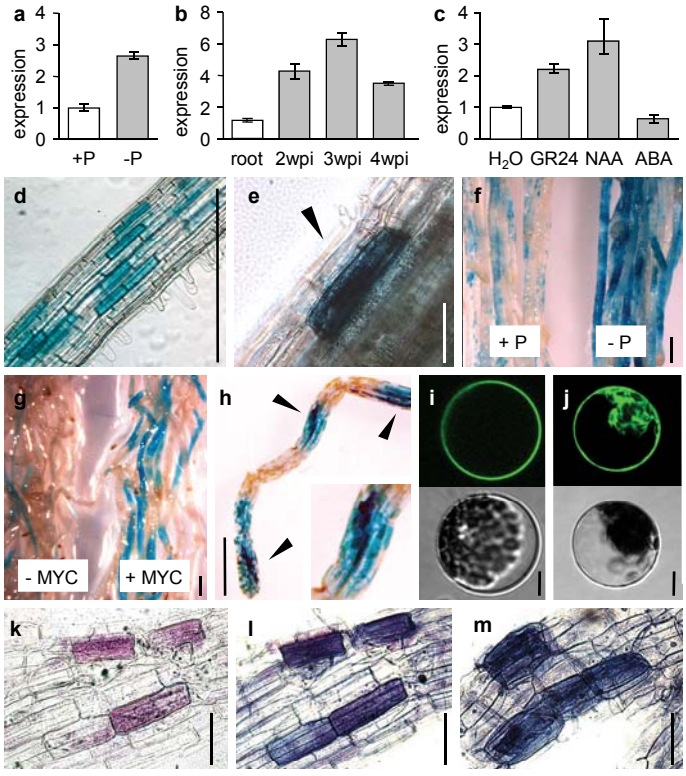
a
b
c
expression
+P
-P
root
2wpi
3wpi
4wpi
H2O
GR24
NAA
ABA
d
e
f
+ P
- P
g
h
i
j
- MYC
+ MYC
k
l
m

Figure 4

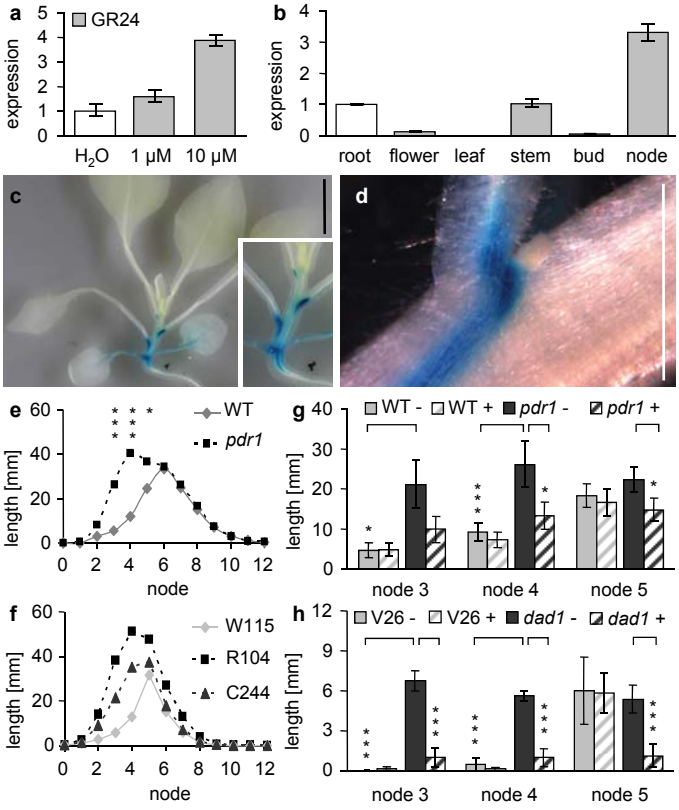
a
GR24
expression
H2O
1 µM
10 µM
b
expression
root
flower
leaf
stem
bud
node
c
d
e
WT
pdr1
length [mm]
node
f
W115
R104
C244
length [mm]
node
g
WT -
WT +
pdr1 -
pdr1 +
length [mm]
node 3
node 4
node 5
h
V26 -
V26 +
dad1 -
dad1 +
length [mm]
node 3
node 4
node 5

Figure 2

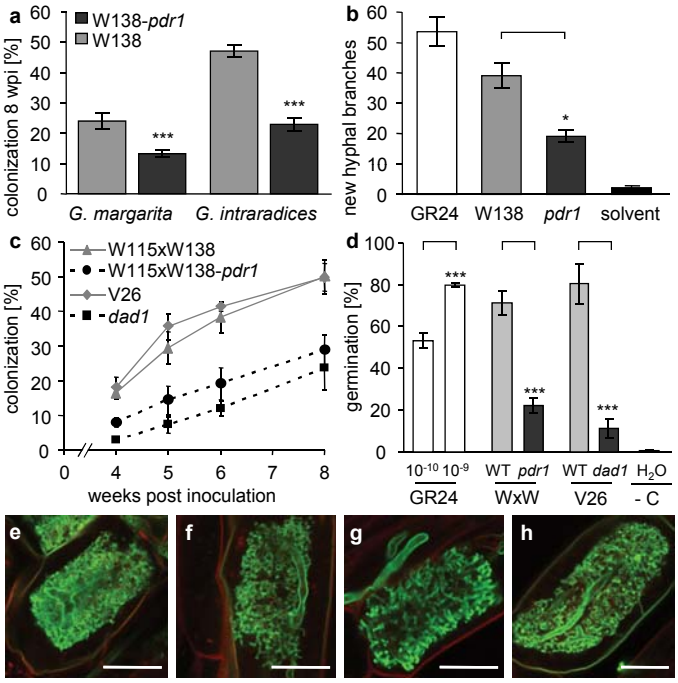
a
W138-pdr1
W138
colonization 8 wpi [%]
***
***
G. margarita
G. intraradices
b
new hyphal branches
*
GR24
W138
pdr1
solvent
c
W115xW138
W115xW138-pdr1
V26
dad1
colonization [%]
weeks post inoculation
d
germination [%]
***
***
***
10-10 10-9
WT pdr1
WT dad1
H2O
GR24
WxW
V26
- C
e
f
g
h

Figure 3

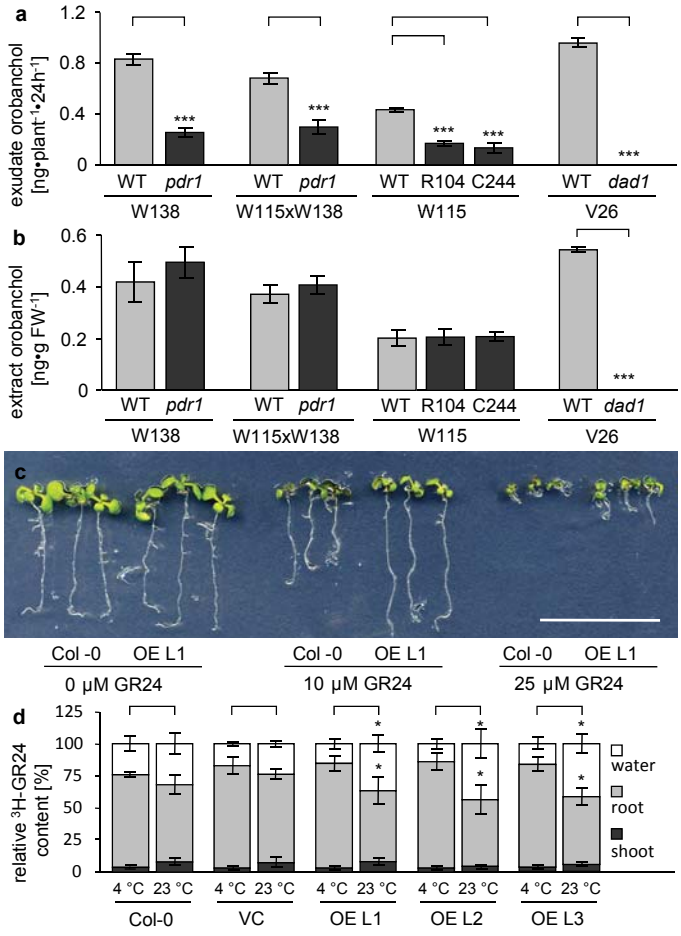
a
exudate orobanchol [ng•plant-1•24h-1]
1.2
0.8
0.4
0
***
WT pdr1 WT pdr1 WT R104 C244 WT dad1
W138 W115xW138 W115 V26
b
extract orobanchol [ng•g FW-1]
0.6
0.4
0.2
0
***
WT pdr1 WT pdr1 WT R104 C244 WT dad1
W138 W115xW138 W115 V26
c
Col -0 OE L1 Col -0 OE L1 Col -0 OE L1
0 µM GR24 10 µM GR24 25 µM GR24
d
relative 3H-GR24 content [%]
125
100
75
50
25
0
water
root
shoot
4 °C 23 °C 4 °C 23 °C 4 °C 23 °C 4 °C 23 °C 4 °C 23 °C
Col-0 VC OE L1 OE L2 OE L3